Chemical Science

Accepted Manuscript

This article can be cited before page numbers have been issued, to do this please use: Y. Liu, X. Lin, J. Deng, Y. Lyu, P. Qian, Y. Li and S. Wang, *Chem. Sci.*, 2018, DOI: 10.1039/C7SC05246D.




ROYAL SOCIETY OF CHEMISTRY

rsc.li/chemical-science

View Article Online
DOI: 10.1039/C7SC05246D

Journal Name

ARTICLE

# Multiple advanced logic gates made of DNA-Ag nanocluster and the application for intelligent detection of pathogenic bacterial genes

Received 00th January 20xx,
Accepted 00th January 20xx

DOI: 10.1039/x0xx00000x

www.rsc.org/

Xiaodong Lin,[a] Yaqing Liu,*[a] Jiankang Deng,[a] Yanlong Lyu,[a] Pengcheng Qian,[a] Yunfei Li,[a] and Shuo Wang*[ab]

Integration of multiple DNA logic gates on a universal platform to implement advance logic functions is a critical challenge for DNA computing. In the present investigation, a straightforward and powerful strategy of guanine-rich DNA sequence lighting up silver nanocluster and fluorophore was developed to construct a library of logic gates on a simple DNA-templated silver nanoclusters (DNA-AgNCs) platform. This library included basic logic gates, YES, AND, OR, INHIBIT, XOR, which were further integrated into complex logic circuits to implement diverse advanced arithmetic/non-arithmetic functions including half-adder, half-subtractor, multiplexer, and demultiplexer. Under UV irradiation, all logic functions could be instantly visualized, confirming excellent repeatability. The logic operations were entirely based on DNA hybridization in an enzyme-free and label-free condition, avoiding waste accumulation and reducing cost consumption. Interestingly, DNA-AgNCs based multiplexer was for the first time used as intelligent biosensor to identify pathogenic genes, *E. coli* and *S. aureus* genes, with high sensitivity. The investigation provides a prototype for wireless integration of multiple devices on even the simplest single-strand DNA platform to perform diverse complex functions in a straightforward and cost-effective way.

## Introduction

To fulfil demands of increased computational complexity, it is critical to integrate multiple logic gates into advanced logic circuits on a universal platform for next generation of molecular computing.[1-3] In electronics, higher-ordered logic circuits implement complex functional and information processing at varying degrees of complexity by electrically wiring multiple required logic gates, which is a significant challenge on a molecular scale.[4] Thanks to massive parallel computation ability, programmable sequence, and predictable configuration, DNA has been validated as an extremely powerful material for the engineering of DNA logic gates.[5-8] To date, various DNA logic gates have been successfully constructed to implement versatile functions from data to information processing.[9-18] According to special catalysis of DNAzymes on many reactions parallel gate arrays, multilayered gate cascades and fan-out gates have been successfully constructed.[19-23] A toe-hold strategy based on entropy-driven DNA strand displacement provides an outstanding possibility for building enzyme-free DNA logic gates.[24,25] Three DNA logic gates (one AND and two NOT) were integrated on a 2D platform via DNA crossover tile technology.[3] The investigations significantly improve the development of DNA computing. However, it is worthy of noting that by products are usually generated during logic operation, resulting in waste accumulation within the system. Meanwhile, cost effective molecular logic gates constructed on a universal platform and featured simple operation still is a main challenge for integration of molecular devices.[26,27]

DNA-templated silver nanoclusers (DNA-AgNCs) with molecular-like properties have attracted increasing attention from extensive research fields due to their intrinsic merits such as excellent photostability, biocompatibility, and low cost.[28] As signal transducer, DNA-AgNCs presents advantages over organic dyes and quantum dots in that the use of DNA-AgNCs not only avoids the covalent label of DNA with a signal indicator, but also makes it easier to be introduced into DNA logic system via the DNA template.[29,30] The fluorescence emission of DNA-AgNCs exhibits size and sequence-dependent property[31] and is highly sensitive to their micro-environment.[32,33] These intrinsic properties endow DNA-AgNCs promising applications in development of parallel/cascade logic gates and computing circuits. Here, we demonstrated that a set of basic logic gates (YES, AND, OR, XOR, and INHIBIT (INH)) and advanced logic gates (half adder (HA), half subtractor (HS), multiplexer (MUX), and demultiplexer (DMUX) could be integrated into a simple

[a] Key laboratory of Food Nutrition and Safety (Ministry of Education), College of Food Engineering and Biotechnology, Tianjin University of Science and Technology, Tianjin 300457, China.
[b] Tianjin Key Laboratory of Food Science and Health, School of medicine, Nankai University, Tianjin 300071, China.
*E-mail: yaqingliu@tust.edu.cn, wangshuo@nankai.edu.cn
Electronic Supplementary Information (ESI) available: [details of any supplementary information available should be included here]. See DOI: 10.1039/x0xx00000x

View Article Online
DOI: 10.1039/C7SC05246D




DNA-AgNCs platform to implement arithmetic and non-arithmetic logic functions.

Aside from the engineering of DNA computing, construction of DNA logic gate is of scientific interesting for intelligent biosensing and diagnostics.[34-37] Up to date, most of the logic-related analyses have been developed according to AND or OR logic gates with biomarkers as inputs.[38,39] An AND gate based diagnosis system reports a high output signal in the coexistence of all biomarkers. For OR gate based detection, any one of the biomarkers can cause a high output signal response. This provides a convincing way for intelligent diagnosis on certain degree. However, AND or OR gate-based analysis suffers from the limitation of distinguishing biomarkers from each other, which might be overcome by a multiplexer gate-based biosensor. With two disease-related foodborne pathogen genes as inputs, here, a 2:1 multiplexer was demonstrated for the first time to act as intelligent biosensor to distinguish each of the genes with one output signal response under logic control.

## Result and discussion

DNA-AgNCs was designed as the universal platform for construction of multiple advanced logic gates, which contained two segments: a cytosine-rich (C-rich) segment for synthesizing AgNCs and an input-recognizing segment. A dim fluorescence of DNA-AgNCs could be lightened up by the approached guanine-rich (G-rich) DNA strand (See Fig. S1 in the supporting information (SI)), which was consistent with previous reports.[40] This implemented the simplest YES gate function. Via simple modulation of input sequences, a set of basic logic gates including XOR, AND, OR, and INH were successfully constructed on the same DNA-AgNCs platform (see Fig. S2-Fig. S8 in SI). Their combinations provide a powerful application to transfer basic Boolean logic gate into advanced logic gates, thus implementing functions of almost the whole family of logic gates.[41-43] Here, we demonstrated that arithmetic functions, such as half adder and half subtractor, and non-arithmetic functions, such as multiplexer and demultiplexer, could be reached by integrating the required basic logic gates on the universal platform of DNA-AgNCs.

As important logic gates, half adder and half subtractor are highly demanded in numerical data and information processing.[44] A half adder can implement an addition function on two binary digits by integrating an XOR gate and an AND gate in parallel to respectively code for a SUM and a CARRY digit, which requires two distinct output signals. Here, fluorescent AgNCs modulated by G-rich DNA sequences was used as signal indicator for the XOR logic gate. Interestingly, G-rich oligonucleotide sequences could form a G-quadruplex (G4) configuration to enhance the fluorescence of organic dyes.[45,46] Such a combination of G-rich DNA modulating fluorescence of AgNCs and fluorophore endows DNA-AgNCs to be powerful building block for construction of advanced logic gates. To implement HA function, NMM (N-Methyl Mesoporphyrin IX) was selected as signal indicator of the required AND gate since it has the properties of special structural selectivity for G4 rather than single, duplexes, or triplexes DNA strands.[47] The resulted complex of G4/NMM can generate a pronounced fluorescent signal.[48,49] Fig. 1A outlines the operation principle of the developed HA. Both AgNCs and NMM emitted dim fluorescence signals in the absence of any input (Fig. 1B, (a) and (e), respectively). Each of the two inputs, $IN1_{HA}$ and $IN2_{HA}$, contained a G-rich segment of (GGGTGGGTGGGT) at the 3'-terminal to augment fluorescence of AgNCs by forming duplexes of DNA-AgNCs/$IN1_{HA}$ and DNA-AgNCs/$IN2_{HA}$ (Fig. 1B, (b) and (c)). In contrast, low fluorescence responses of NMM were monitored in both cases where the G-rich sequence of (GGGTGGGTGGGT) in $IN1_{HA}$ and $IN2_{HA}$ could not form G4 configuration and thus had no significant influence on the fluorescence of NMM (Fig. 1B, (f) and (g), respectively). When both inputs coexist, they preferred to hybridize together while did not hybridize with DNA-AgNCs. Then, AgNCs reported a dim fluorescence signal (Fig. 1B, (d)). However, the fluorescence of NMM was strongly augmented (Fig. 1B, (h)) since the G-rich sequence of (GGGTGGGTGGGT) at the 3'-terminal of $IN1_{HA}$ formed a G4 configuration by hybridizing with the (TGGGT) sequence at the 5'-terminal of $IN2_{HA}$, which further formed the G4/NMM complex. The formation of the G4 configuration was validated by circular dichroism (CD) experiments (Fig. S9 in SI). The DNA interactions were validated by native polyacrylamide gel electrophoresis (PAGE) experiment (Fig. S10 in SI).

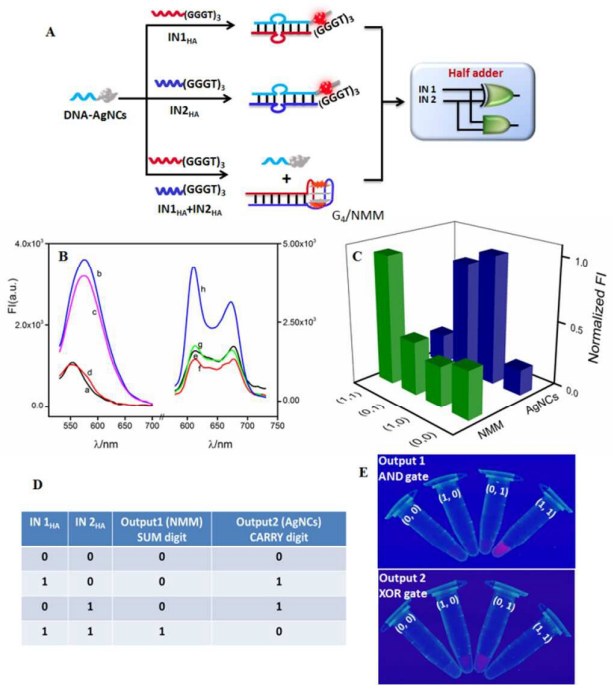


| $IN\ 1_{HA}$ | $IN\ 2_{HA}$ | Output1 (NMM) SUM digit | Output2 (AgNCs) CARRY digit |
|---|---|---|---|
| 0 | 0 | 0 | 0 |
| 1 | 0 | 0 | 1 |
| 0 | 1 | 0 | 1 |
| 1 | 1 | 1 | 0 |

**Fig. 1** (A) The principle scheme of the developed half adder and the corresponding logic gate. (B) Results of half adder: the fluorescent responses of DNA-AgNCs (left) and NMM (right) against the input combinations, in the absence of inputs (a, e) and in the presence of $IN1_{HA}$ (b, f), $IN2_{HA}$ (c, g), and $IN1_{HA}$+$IN2_{HA}$ (d, h). (C) The $FI_{max(NMM)}$ and $FI_{max(AgNCs)}$ against various input combinations. The corresponding truth table (D) and photographs of the half adder under UV irradiation (E).

To implement HA function, the normalized fluorescence intensities of signal indicator at maximum peak, $FI_{max(NMM)}$ and

View Article Online
DOI: 10.1039/C7SC05246D




$FI_{max(AgNCs)}$ were plotted as a function of input combinations (Fig. 1C). Similar to the approach used in electronics, the output signal with an undefined range was defined as "1" or "0" when the normalized fluorescence intensity was higher than 0.45 or lower than 0.4, respectively. This definition was available for all logic operations in this work. The resulted truth table (Fig. 1D) clearly demonstrated that AND and XOR gates were successfully integrated in parallel to implement the HA arithmetic function. The entire logic system executes binary arithmetic operations of (0 + 0 = 0 0), (1 + 0 = 0 1), and (0 + 1 = 0 1). The case of (1+ 1=2) endowed the SUM digit as 0 and the CARRY digit as 1, yielding (1 + 1 = 1 0).[50] Interestingly, the HA logic operation could be directly observed from the photos of the AND and XOR logic gates under UV irradiation (Fig. 1E). The fluorescence of NMM could be directly visualized in the coexistence of the two inputs, corresponding to the AND gate operation. For the XOR gate, the fluorescence of DNA-AgNCs could be clearly observed in the presence of either $IN1_{HA}$ or $IN2_{HA}$. The results matched the fluorescence results quite well, validating the excellent reproducibility of the logic operations. Noteworthy, the developed integration strategy of molecular device presents advantages that the required AND and XOR gate share a common threshold value, a universal platform and the same set of inputs. Furthermore, the use of NMM as the second signal indicator by combining G-rich sequence modulation has advantages of avoiding chemical label and simplifying logic operations. This also provides an instructive strategy to wirelessly integrate molecular devices on a universal platform for untraditional molecular computing with simple operation. This successful integration inspired us to construct other advanced logic gates on the DNA-AgNCs platform.

A half subtractor can implement a subtraction function of two bits by combining an XOR gate and an INH gate in parallel to produce a DIFFERENCE bit and a BORROW bit, respectively.[51] Different from HA, an INH gate while not AND gate is required by HS to integrate with an XOR gate. By modulating the input DNA sequences, an INH gate could be feasibly integrated with the developed XOR gate on the DNA-AgNCs platform. Fig. 2A outlines the operation principle of the as-developed HS. Both AgNCs and NMM reported low fluorescence signal at the initial state, respectively (Fig. 2B, (a) and (e)). $IN1_{HS}$ containing G-rich sequence (GGGTGGGTGGGTGGGT) at the 3'-terminal and $IN2_{HS}$ containing G-rich sequence (GGGTGGGTGGGT) at the 3'-terminal could light up fluorescence of AgNCs by forming duplex of DNA-AgNCs/$IN1_{HS}$ (Fig. 2B, (b)) and DNA-AgNCs/$IN2_{HS}$ (Fig. 2B, (c)), respectively. The coexistence of the two inputs produced duplex of $IN1_{HS}$/$IN2_{HS}$ due to the stronger affinity between $IN1_{HS}$ and $IN2_{HS}$, leaving DNA-AgNCs alone with low fluorescence response (Fig. 2B, (d)). For the NMM-related INH gate, the G-rich sequence (GGGTGGGTGGGTGGGT) of $IN_{HS}$ outstandingly enhanced the fluorescence of NMM by forming a G4/NMM complex (Fig. 2B, (f)). The guanine base sequence (GGGTGGGTGGGT) at the 3'-terminal of $IN2_{HS}$, however, was not sufficient to form a G4 configuration, producing a low fluorescence of NMM (Fig. 2B, (g)). In the coexistence of the two inputs, the C-rich segment (CCCACCC) at the 5'-terminal of $IN2_{HS}$ hybridized with the G-rich segment at the 3'-terminal of $IN1_{HS}$, inhibiting the formation of G4. Therefore, no enhanced fluorescence of NMM was monitored (Fig. 2B, (h)). The modulation of the G4 configuration was validated by CD experiments (Fig. S11 in SI).

By plotting $FI_{max(NMM)}$ and $FI_{max(AgNCs)}$ against input combinations (Fig. 2C), the resulted truth table (Fig. 2D) indicates that the NMM-related INH logic gate and the AgNCs-related XOR logic gate respectively performed the BORROW and DIFFERENT functions. The whole logic system implements binary arithmetic operations of (0 - 0 = 0 0), (1 - 0 =0 1), and (1 - 1 = 0 0). The case of (0 - 1) is calculated via high borrow to transfer it to (2 - 1=1), endowing both BORROW and DIFFERENT digits as "1" and finally getting the result of (0 - 1= 1 1).[50] Thus, the half subtractor was successfully achieved by integrating XOR and INH logic gates in parallel on a simple platform by hybridizing with two single strand DNA inputs in an enzyme-free and waste-free way. Fig. 2E exhibits the respective visions of INH and XOR logic operations under UV irradiation. The results further validate the reproducibility and reliability of the designed logic gate.

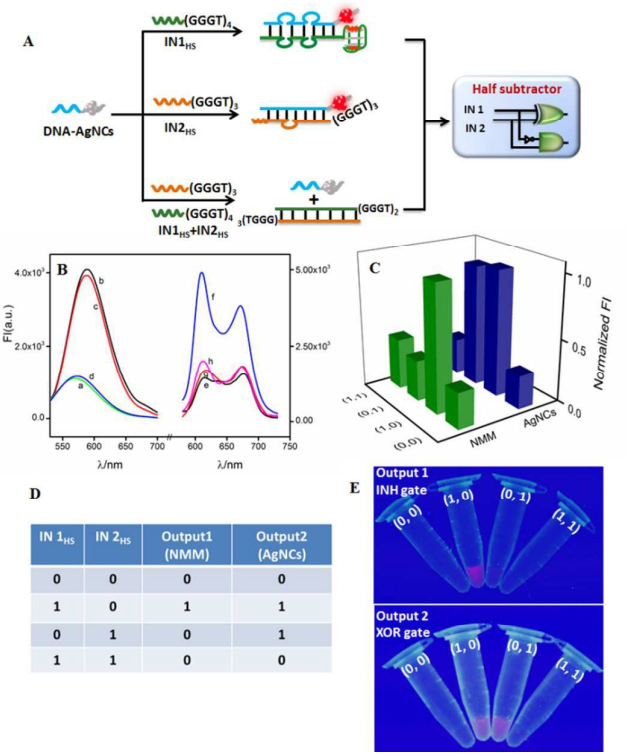


| $IN1_{HS}$ | $IN2_{HS}$ | Output1 (NMM) | Output2 (AgNCs) |
|---|---|---|---|
| 0 | 0 | 0 | 0 |
| 1 | 0 | 1 | 1 |
| 0 | 1 | 0 | 1 |
| 1 | 1 | 0 | 0 |

**Fig. 2** (A) The operation principle of the developed half subtractor and the corresponding logic gate. (B) Results of half subtractor: the fluorescent responses of DNA-AgNCs (left) and NMM (right) against various input combinations, in the absence of inputs (a, e) and in the presence of $IN1_{HS}$ (b, f), $IN2_{HS}$ (c, g) and $IN1_{HS}$+$IN2_{HS}$ (d, h). (C) The $FI_{max(NMM)}$ and $FI_{max(AgNCs)}$ against input combinations. The corresponding truth table (D) and photographs of the half subtractor under UV irradiation (E).

The developed half adder and half subtractor belong to the category of arithmetic logic gate. Molecular computing requires logic gates not only for arithmetic operations, but also for non-arithmetic operations such as data transmission and

View Article Online
DOI: 10.1039/C7SC05246D




compression/decompression, which are critical for information theory and computer science, while these have rarely been developed on a molecular scale.[50] This inspired us to further construct non-arithmetic logic gates such as multiplexer (MUX) and demultiplexer (DMUX) on the DNA-AgNCs platform. Both multiplexer and demultiplexer consist of input, selector, and output, implementing data decompression and compression functions under selector control.[52] A 1:2 DMUX can transmit one input ($IN_{DMUX}$) into two output channels via a selector ($S_{DMUX}$) control, which could be realized by integrating an AND gate and an INH gate in parallel. As illustrated in Fig. 3A, the required AND logic gate with NMM as signal indicator was integrated with AgNCs-related INH gate on the DNA-AgNCs platform to implement a demultiplexer function. Both AgNCs and NMM exhibited low fluorescence in the absence of $IN_{DMUX}$ and $S_{DMUX}$ (Fig. 3B, (a) and (e), respectively). The $IN_{DMUX}$ could hybridize with the input-recognition segment of DNA-AgNCs, forming a duplex of DNA-AgNCs/$IN_{DMUX}$. The G-rich sequence (GGGTGGGTGGGT) at the 3'-terminal of $IN_{DMUX}$ was then approached to the AgNCs at the 5'-terminal of DNA-AgNCs, lighting up the fluorescence of AgNCs (Fig. 3B, (b)). However, the G-rich sequence (GGGTGGGTGGGT) could not form G4 configuration, generating a low fluorescence of NMM (Fig. 3B, (f)). The $S_{DMUX}$ contained the sequence of (GGGT) at the 5'-terminal, which was designed to neither hybridize with DNA-AgNCs nor form G4 configuration. Thus, neither the fluorescence of AgNCs (Fig. 3B, (c)) nor the fluorescence of NMM (Fig. 3B, (g)) was enhanced. In the coexistence of $IN_{DMUX}$ and $S_{DMUX}$, duplex of $IN_{DMUX}$/$S_{DMUX}$ rather than DNA-AgNCs/$IN_{DMUX}$ was generated due to the higher affinity between $IN_{DMUX}$ and $S_{DMUX}$, resulting in a low fluorescence of DNA-AgNCs (Fig. 3B (d)). However, the formation of $IN_{DMUX}$/$S_{DMUX}$ gathered the G-rich sequence (GGGTGGGTGGGT) at the 3'-terminal of $IN_{DMUX}$ and (GGGT) at the 5'-terminal of $S_{DMUX}$ together to generate G4 configuration, leading to an outstanding fluorescence of NMM (Fig. 3B (h)). Therefore, the $IN_{DMUX}$ was transmitted into channel 2 in the presence of $S_{DMUX}$. By plotting the output channels of $FI_{max(NMM)}$ and $FI_{max(AgNCs)}$ against the input combinations (Fig. 3C), the demultiplexer operation could be conveniently obtained from the truth table (Fig. 3D). This can be instantly visualized from the photographs under UV irradiation (Fig. 3E). The input was transmitted into channel 1 with AgNCs as signal indicator if the selector ($S_{DMUX}$) kept "OFF". Otherwise, the $IN_{DMUX}$ was transmitted into channel 2 with NMM as signal indicator.

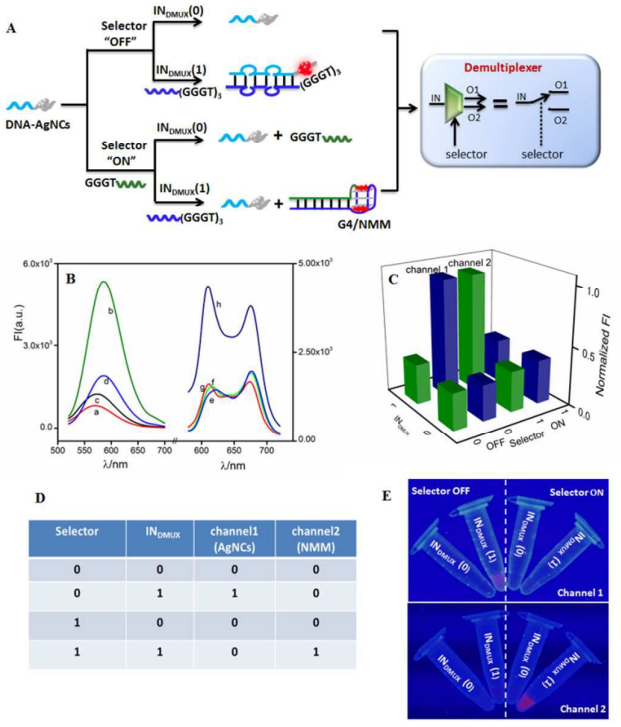


| Selector | $IN_{DMUX}$ | channel1 (AgNCs) | channel2 (NMM) |
|---|---|---|---|
| 0 | 0 | 0 | 0 |
| 0 | 1 | 1 | 0 |
| 1 | 0 | 0 | 0 |
| 1 | 1 | 0 | 1 |

**Fig. 3** (A) The operation principle of the developed 1:2 demultiplexer and the corresponding logic gate. (B) Results of 1:2 demultiplexer: the fluorescent responses of DNA-AgNCs (left) and NMM (right) against various input combinations, in the absence of inputs (a, e) and in the presence of $IN1_{DMUX}$ (b, f), $S_{DMUX}$ (c, g) and $IN1_{DMUX}$+$S_{DMUX}$ (d, h). (C) The $FI_{max(NMM)}$ and $FI_{max(AgNCs)}$ against various input combinations. The corresponding truth table (D) and photographs of the 1:2 demultiplexer under UV irradiation (E).

A 2:1 multiplexer (MUX) executes a reversed function to the 1:2 demultiplexer, which consists of two inputs, one selector and one output channel. By controlling the selector in "ON" or "OFF" state, the two inputs can be selectively transmitted into a single output channel.[53] Fig. 4A depicts the operation principle of the developed 2:1 MUX with AgNCs as signal reporter. Here, we first discussed the case in the absence of $S_{MUX}$, *i.e.*, when the selector kept "OFF". The original logic system reported a dim fluorescence signal in the absence of both inputs ($IN1_{MUX}$ and $IN2_{MUX}$), Fig. 4B (a). Both $IN1_{MUX}$ and $IN2_{MUX}$ contained G-rich segments. The $IN1_{MUX}$ could hybridize with the DNA-AgNCs, thus transforming the AgNCs into bright-fluorescence-emitting clusters by the approached G-rich segment, Fig. 4B (b). In contrast to $IN1_{MUX}$, $IN2_{MUX}$ did not hybridize with DNA-AgNCs, resulting in a low output signal, Fig. 4B (c). In the coexistence of $IN1_{MUX}$ and $IN2_{MUX}$, $IN2_{MUX}$ had no influence on the hybridization between $IN1_{MUX}$ and DNA-AgNCs. A high output signal was then monitored, which was similar as that in the presence of only $IN1_{MUX}$, Fig. 4B (d). The results demonstrate that the multiplexer would report a high output signal of "1" in the presence of $IN1_{MUX}$ and a low output signal of "0" in the absence of $IN1_{MUX}$, which was independent of the presence or absence of $IN2_{MUX}$ if the selector was absent. Considering the other case that the selector was in the state of "ON", the added $S_{MUX}$ would associate with DNA-AgNCs to form a duplex of DNA-AgNCs/$S_{MUX}$, which still reported a low output signal (Fig. 4B, (e)). Here, DNA-AgNCs was designed to have higher affinity to $S_{MUX}$ than to $IN1_{MUX}$. Therefore, the addition of $IN1_{MUX}$ had no obvious influence on the duplex formation of $S_{MUX}$/DNA-AgNCs. A low output signal would then be monitored (Fig. 4B, (f)). In the addition of $IN2_{MUX}$, the $S_{MUX}$ would act as linker, bringing $IN2_{MUX}$ and DNA-AgNCs together. The approached G-rich segment of $IN2_{MUX}$ significantly enhanced the fluorescence of the AgNCs (Fig. 4B, (g)). A similar augmented fluorescence signal was detected in the coexistence of $S_{MUX}$, $IN1_{MUX}$, and $IN2_{MUX}$ (Fig. 4B, (h)), since $IN1_{MUX}$ also had no influence on the association among $IN2_{MUX}$, $S_{MUX}$, and DNA-AgNCs. Apparently, the multiplexer would report a high output signal in the presence of $IN2_{MUX}$ and a low output

View Article Online
DOI: 10.1039/C7SC05246D




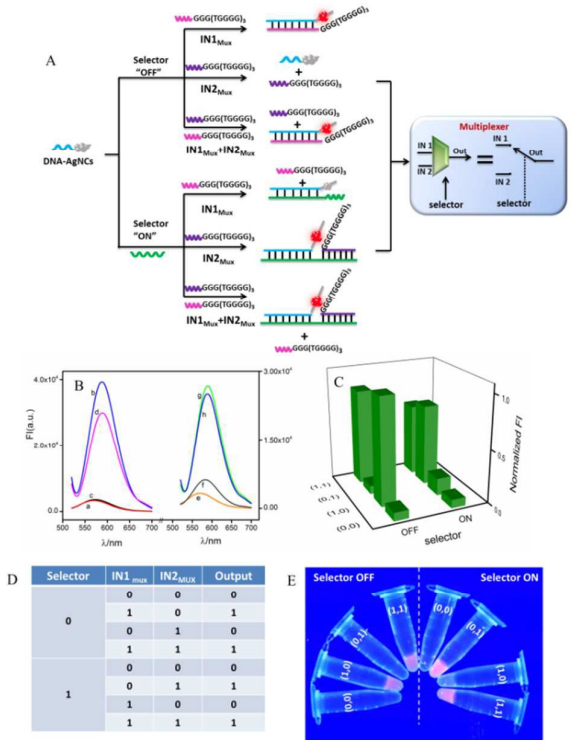


| Selector | $IN1_{MUX}$ | $IN2_{MUX}$ | Output |
|---|---|---|---|
| 0 | 0 | 0 | 0 |
| | 1 | 0 | 1 |
| | 0 | 1 | 0 |
| | 1 | 1 | 1 |
| 1 | 0 | 0 | 0 |
| | 0 | 1 | 1 |
| | 1 | 0 | 0 |
| | 1 | 1 | 1 |

**Fig. 4** (A) The principle scheme of the developed 2:1 multiplexer and the corresponding logic gate. (B) Results of 2:1 multiplexer: the fluorescent responses of DNA-AgNCs (a), in the presence of $IN1_{MUX}$ (b), $IN2_{MUX}$ (c) and $IN1_{MUX}$+$IN2_{MUX}$ (d), $S_{MUX}$ (e), $S_{MUX}$+$IN1_{MUX}$ (f), $S_{MUX}$+$IN2_{MUX}$ (g). (C) The $FI_{max}$ of DNA-AgNCs against various input combinations. The corresponding truth table (D) and photographs of the 2:1 multiplexer under UV irradiation (E).

signal in the absence of $IN2_{MUX}$ no matter of absence or presence of $IN1_{MUX}$ if the selector was kept at "OFF". The plotting of $FI_{MAX}$ against input combinations (Fig. 4C) generated the corresponding truth table (Fig. 4D), which was further validated by the photographs of the multiplexer operation, triggered by UV irradiation (Fig. 4E). These results demonstrate that the multiplexer would transfer the state of $IN1_{MUX}$ into the output channel if keeping the selector "OFF". It would transmit the state of the $IN2_{MUX}$ into the output channel if keeping the selector "ON". This meets the feature of a 2:1 multiplexer.

Up to now, arithmetic logic gates of HA and HS and non-arithmetic logic gates of MUX and DMUX have been successfully constructed on the universal platform of DNA-AgNCs. Considering the reuse of the developed logic gates, resetting the logic system would be a possible way which could be realized by modifying the DNA-AgNCs on magnetic nanoparticle surface (MNP/DNA-AgNCs). After finishing the logic operations, the logic system was heated at 90oC for 10 min to de-hybridize the formed DNA duplexes. Under the assistant of magnetic field, the MNP/DNA-AgNCs would be separated from the released DNA strands, which was then used to implement the next cycle of logic operations.

Except for data and information processing, the developed DNA logic system as intelligent biosensor was further explored. As dangerous pathogenic bacteria, Escherichia coli (*E. coli*) and Staphylococcus aureus (*S. aureus*) can cause foodborne infectious and seriously threaten public health.[54] Here, *E. coli* gene and *S. aureus* gene were used as model targets to validate the logic-controlled detection via multiplexer function. To realize 2:1 multiplexer-based intelligent detection, a G-rich DNA strand (G-DNA) and two DNA strands-templated AgNCs ($P_1$-AgNCs and $P_2$-AgNCs) were designed as the platform, which was illustrated in Fig. 5. Here, we first discussed the case in the absence of the selector DNA (S-DNA). The IN1 of *S. aureus* gene acted as linker to bridge $P_1$-AgNCs and G-DNA together to form complex of IN1/$P_1$-AgNCs/G-DNA. The dim fluorescence of AgNCs (Fig. 6A, (a)) was significantly enhanced by the approached G-DNA (Fig. 6A, (b)). In the presence of IN2, *E. coli* gene, it would hybridize with $P_2$-AgNCs and form duplex of IN2/$P_2$-AgNCs, which had no influence on the fluorescence of AgNCs (Fig. 6A, (c)). In the coexistence of IN1 and IN2, IN1/$P_1$-AgNCs/G-DNA and IN2/$P_2$-AgNCs were generated, resulting in an enhanced fluorescence output signal (Fig. 6A, (d)). The results demonstrate that the multiplexer would report a high output signal of "1" in the presence of *S. aureus* gene and a low output signal of "0" in the absence of *S. aureus* gene, which was independent of the presence or absence of *E. coli* gene if the selector kept "OFF".

In the addition of S-DNA, the IN1 of *S. aureus* gene would hybridize with the S-DNA rather than with $P_1$-AgNCs and G-DNA due to the higher affinity between IN1 and S-DNA. A low output signal similar as the original fluorescence (Fig.6A, (e)) was then monitored (Fig. 6A, (f)). Different from that, IN2 of *E. coli* gene would link $P_2$-AgNCs and S-DNA together, forming complex of IN2/$P_2$-AgNCs/S-DNA. The AgNCs of $P_2$-AgNCs approached to the G-rich sequence of S-DNA, producing an augmented fluorescence signal of AgNCs (Fig. 6A, (g)). In the coexistence of IN1 and IN2, IN1 would hybridize with S-DNA, which had no influence on the hybridization among IN2, $P_2$-AgNCs and S-DNA, resulting in an enhanced output signal (Fig. 6A, (h)). Obviously, the multiplexer would report a high output signal in

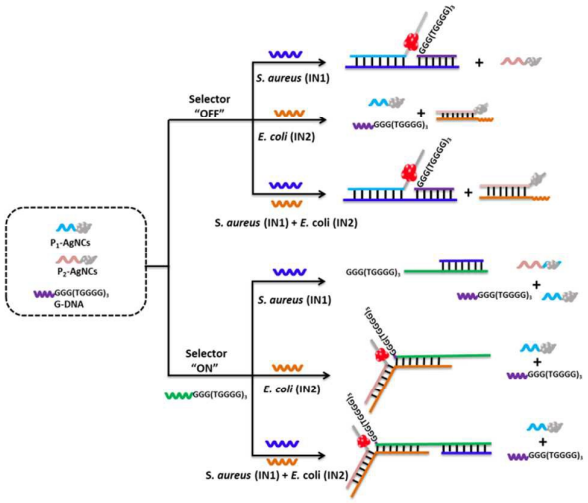


**Fig. 5** The principle scheme of multiplexer-controlled intelligent detection of pathogenic bacterial gene. In the absence of selector DNA, the 2:1 multiplexer would transfer the *S. aureus* gene into the output channel. In the presence of selector DNA, the 2:1 multiplexer would transfer the *E. coli* gene into the output channel.

View Article Online
DOI: 10.1039/C7SC05246D




the presence of *E. coli* gene and a low output signal in the absence of *E. coli* gene, which was independent of the presence or absence of *S. aureus* gene if the selector was kept "ON". By plotting the normalized fluorescence of the AgNCs against various input combinations (Fig. 6B), the results demonstrate that the multiplexer would transfer the state of *S. aureus* gene into the output channel if keeping the selector "OFF" and would transmit the state of *E. coli* gene into the output channel if the selector was switched "ON". Meanwhile, limit of detection reaches 100 fM for both *E. coli* and *S. aureus* genes detection due to the G-rich enhancement on the fluorescence of AgNCs (See Fig. S12 in SI).

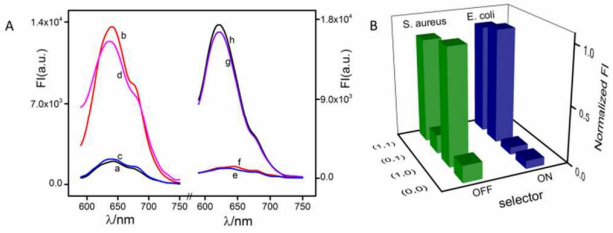


**Fig. 6** (A) The fluorescence responses of the 2:1 multiplexer in the absence of S-DNA (Left) and in the presence of S-DNA (Right) against various input combinations, in the absence of the two inputs (a, e), in the presence of IN1 (b, f), in the presence of IN2 (c, g), in the presence of IN1 and IN2 (d, h). (B) Fluorescence intensity of the multiplexer at $FI_{max}$ against *S. aureus* and *E. coli* genes under selector function.

Such a design enables to identify multiple targets with a single signal indicator and also could help to make a rapid evaluation on various states of input in the sample.[55] As illustrated in Table 1, the 2:1 multiplexer-based sensing system in the presence of the selector DNA was defined as detection kit A. The sensing system in the absence of the selector DNA was defined as detection kit B. For the decision making, the sample was divided into two parts and added into the kit A and kit B, respectively. If both detection kit A and kit B reported low output signal ("0"), then, neither *S. aureus* nor *E. coli* gene existed in the sample. If a high output ("1") was detected from kit A, indicating the existence of *E. coli*. The high output ("1") of kit B suggested the presence of *S. aureus*. If both kits reported high output ("1"), then, the sample contained both *S. aureus* and *E. coli*. The multiplexer-based biosensing system simplifies the operation effort and reduces the assay time, presenting great potential application in high-throughput rapid detection.

**Table 1** 2:1 Multiplexer-based biosensing system for rapid analysis of pathogenic genes

| Output of detection kit A (with the S-DNA) | Output of detection kit B (without the S-DNA) | Rapid decision-making |
|---|---|---|
| 0 | 0 | Containing nether *S. aureus* nor *E. coli* |
| 1 | 0 | Containing *E. coli* |
| 0 | 1 | Containing *S. aureus* |
| 1 | 1 | Containing both *S. aureus* and *E. coli* |

## Conclusions

We have successfully developed a novel strategy for the wireless integration of DNA logic gates into a simple and universal platform to implement multiple advanced arithmetic and non-arithmetic logic functions. To the best of our knowledge, this is the first time that a library of basic logic gates (YES, AND, OR, XOR and INH) and advanced logic gates (half adder, half subtractor, multiplexer and demultiplexer) have been constructed on the simplest single-strand DNA platform. The repeatability was further validated by instantly visualizing the logic operation under UV irradiation. All the logic gates shared a common threshold value, which would be beneficial for the integration of multiple molecular devices. The strategy of G-rich DNA sequence lighting up AgNCs and NMM for generating output signal avoids the chemical labeling of fluorophore and quencher, providing a cost-effective and powerful way for constructing complex logic gates. The enzyme-free logic operations were quite simple and entirely implemented on the basis of DNA strand-hybridization, thus eliminating waste accumulation in the system and reducing the overall time-consumption of DNA computing. Apart from futuristic vision for molecular computing, the potential application of logic gates for intelligent detection has been further confirmed by distinguishing the *E. coli* and *S. aureus* genes with one output signal under multiplexer control. The developed strategy is straightforward and versatile, thus providing an instructive way for the integration of multiple molecular devices and intelligent diagnosis.

## Conflicts of interest

The authors declare no competing financial interest.

## Acknowledgements

This work is supported by the National Natural Science Foundation of China (No. 21575138 and No. 21775108). China International Science and Technology Cooperation Based of Food Nutrition/Safety and Medicinal Chemistry. The Tianjin Municipal Science and Technology Commission (Project No. 16PTSYJC00130). The International Science and Technology Cooperation Program of China (Project No. 2014DFR30350).

## Experimental details

**The synthesis of DNA-AgNCs**

The DNA-AgNCs were prepared according to previous report.[56] Briefly, $AgNO_3$ solution (6 μM) was added into oligonucleotide solutions (1μM) (phosphate buffer, 20 mM, pH 7.4) and incubated for 30 min at 4℃. $NaBH_4$ solution (6 μM) was then quickly added into the mixture under vigorous shaking. DNA-AgNCs with maximum emission at 620 nm and 580 nm were obtained by modulating the mole ration of DNA, $Ag^+$ and $NaBH_4$ with 1:6:6 and 1:12:6, respectively. The resultant mixture was kept in dark at 4℃.

**Native polyacrylamide gel electrophoresis**

View Article Online
DOI: 10.1039/C7SC05246D




Polyacrylamide gels (20%) were prepared with 1×TBE buffer (pH 8.3). All the used DNAs were denatured by heating at 90 °C for 10 min and then slow cooling down to about 25 °C. Each sample (9 μL) was mixed with loading buffer (1 μL) before loading onto the gel. The gel was run at a constant voltage of 100 V over a period of about 2.5 h. The gel was then immersed in SYBR@Gold Nucleic Acid Gel Stain solution (1X) for about 30 min and then washed with water twice. The gel images were obtained from the Gel Doc™ XR+, Bio-RAD system (USA).

**UV photograph**

The UV photographs of the as-prepared logic gates of YES, AND, OR, INH, XOR, HA, HS, MUX and DMUX were carried out under UV light irradiation with excitation source (365 nm). To take photographs of the advanced logic operations, HA, HS, and DMUX, the signal probes were added individually. NMM was absence when taking photographs for DNA-AgNCs-related logic operations. To directly observe NMM-related logic operations, only the DNA strand of the DNA-AgNCs while not the DNA-AgNCs was used.

**CD Measurement**

A Bio-Logic MOS450 spectropolarimeter (France) was utilized to collect the CD spectra of oligonucleotides (4 μM) at room temperature. An average of three scans from 210 nm to 330 nm was recorded in an optical chamber (1 mm optical path length). The background of the buffer solution (PB buffer, 10 mM, pH 7.4, 10 mM $K^+$) was subtracted from the CD data. Throughout the experiments, the lamp of the spectropolarimeter was always kept under a stable flow of dry purified nitrogen (99.99%) to avoid ozone production.

**Logic operation**

DNA-AgNCs (maximum emission at 580 nm) was used as the platform for all the developed logic operations in this investigation, including YES, AND, OR, INH, XOR, HA, HS, MUX, DMUX. The required inputs with various combinations for each logic gates were added into the logic system according to the logic operation. After incubating 1h at room temperature, the fluorescence spectra of DNA-AgNCs and NMM were recorded. The concentrations of all used DNAs were 500 nM for YES, AND, OR, INH and XOR logic gates. The concentrations of all used DNAs were 200 nM for HA, HS, MUX and DMUX logic gates. The concentration of NMM was 200 nM for HA, HS and DMUX logic gates. All the used DNA strands could be found from Table S1 in supporting information. All used chemicals and materials could be found in SI.

## Supporting Information

Chemicals, materials and DNA sequences used in the investigation, the construction of YES, AND, OR, XOR and INH logic gates, CD and PAGE experimental results.

## Notes and references

1 J. Macdonald, Y. Li, M. Sutovic, H. Lederman, K. Pendri, W. H. Lu, B. L. Andrews, D. Stefanovic and M. N. Stojanovic, *Nano Lett.*, **2006**, 6, 2598-2603.
2 R. Guliyev, S. Ozturk, Z. Kostereli and E. U. Akkaya, *Angew. Chem. Int. Ed.,* 2011, **50**, 9826-9831.
3 Y. V. Gerasimova and D. M. Kolpashchikov, *Angew. Chem. Int. Ed.*, 2016, **55**, 10244-10247.
4 K. S. Park, M. W. Seo, C. Jung, J. Y. Lee and H. G. Park, *Small*, 2012, **8**, 2203-2212.
5 J. B. Zhu, L. B. Zhang, S. J. Dong and E. K. Wang, *ACS Nano*, 2013, **7**, 10211-10217.
6 Y. H. Lin, Y. Tao, F. Pu, J. S. Ren and X. G. Qu, *Adv. Funct. Mater.*, 2011, **21**, 4565-4572.
7 J. Li, A. A. Green, H. Yand and C. H. Fan, *Nat. Chem.,* 2017, **9**, 1056-1067.
8 F. Pu, Z. Liu, J. S. Ren and X. G. Qu, *Chem. Commun.,* 2013, **49**, 2305-2307.
9 F. Wang, C. H. Lu and I. Willner, *Chem. Rev.,* 2014, **114**, 2881-2941.
10 F. Pu, J. S. Ren and X. G. Qu, *Adv. Mater.,* 2014, **26**, 5742-5757
11 M. N. Stojanovic, D. Stefanovic and S. Rudchenko, *Acc. Chem. Res.,* 2014, **47**, 1845-1852.
12 L. M. Adleman, *Science*, 1994, **266**, 1021-1024.
13 H. L. Li, W. Hong, S. J. Dong, Y. Q. Liu and E. K. Wang, *ACS Nano*, 2014, **8**, 2796-2803.
14 L. Qian and E. Winfree, *Science,* 2011, **332**, 1196-1201.
15 J. H. Chen, S. G. Zhou and J. L. Wen, *Angew. Chem. Int. Ed.*, 2015, **54**, 446-460.
16 Y. Tam, Z. W. Dai, M. S. Chan, L. S. Liu, M. C. Cheung, F. Bolze, C. Tin and P. K. Lo, *Angew. Chem. Int. Ed.*, 2016, **55**, 164-168.
17 J. Elbaz, F. Wang, F. Remacle and I. Willner, *Nano Lett.*, 2012, **12**, 6049-6054.
18 H. L. Li, S. J. Guo, Q. H. Liu, L. D. Qin, S. J. Dong, Y. Q. Liu and E. K. Wang, *Adv. Sci.*, 2015, **2**, 1500054.
19 R. J. Pei, E. Matamoros, M. H. Liu, D. Stefanovic and M. Stojanovic, *Nat. Nanotech.*, 2010, **5**, 773-777.
20 R. Orbach, B. Willner and I. Willner, *Chem. Commun.*, 2015, **51**, 4144-4160.
21 C. W. Brown III, M. R. Lakin, E. K. Horwitz, L. Fanning, H. E. West, D. Stefanovic and S. W. Graves, *Angew. Chem. Int. Ed.*, 2014, **53**, 7183-7187.
22 J. Elbaz, O. Lioubashevski, F. Wang, F. Remacle, R. D. Levine and I. Willner, *Nat. Nanotech.*, 2010, **5**, 417-422.
23 R. Orbach, F. Wang, O. Lioubashevski, R. D. Levine and F. Remacle, *Chem. Sci.,* 2014, **5**, 3381-3387.
24 B. M. Frezza, S. L. Cockroft and M. R. Ghadiri, *J. Am. Chem. Soc.*, 2007, **129**, 14875 -14879.
25 J. B. Zhu, L. B. Zhang, T. Li, S. J. Dong and E. K. Wang, *Adv. Mater.*, 2013, **25**, 2440-2444.
26 H. Pei, L. Liang, G. B. Yao, J. Li, Q. Huang and C. H. Fan, *Angew. Chem. Int. Ed.*, 2012, **51**, 9020-9024.
27 A. J. Thubagere, C. Thachuk, J. Berleant, R. F. Johnson, D. A. Ardelean, K. M. Cherry and L. L. Qian, *Nat. Commun.*, 2017, **8**, 14373.
28 E. G. Gwinn, P. O'Neill, A. J. Guerrero, D. Bouwmeester and D. K. Fygenson, *Adv. Mater.*, 2008, **20**, 279-283.
29 D. Q. Fan, J. B. Zhu, Y. Q. Liu, E. K. Wang and S. J. Dong, *Nanoscale*, 2016, **8**, 3834-3840.
30 T. Li, L. B. Zhang, J. Ai, S. J. Dong and E. K. Wang, *ACS Nano*, 2011, **5**, 6334-6338.
31 W. W. Guo, J. P. Yuan, Q. Z. Dong and E. K. Wang, *J. Am. Chem. Soc.*, 2010, **132**, 932-934.
32 H. C. Yeh, J. Sharma, J. J. Han and J. S. Martinez, *Nano Lett.*, 2010, **10**, 3106-3110.
33 N. Enkin, F. Wang, E. Sharon, H. B. Albada and I. Willner, *ACS Nano,* 2014, **8**, 11666-11673.
34 M. X. You, L. Peng, N. Shao, L. Q. Zhang, L. P. Qiu, C. Cui and W. H. Tan, *J. Am. Chem. Soc.*, 2014, **136**, 1256-1259.
35 J. Hemphill and A. Deiters, *J. Am. Chem. Soc.*, 2013, **135**, 10512-10518.

View Article Online
DOI: 10.1039/C7SC05246D


36 Z. Xie, L. Wroblewska, L. Prochazka, R. Weiss and Y. Benenson, *Science*, 2011, **333**, 1307-1311.
37 W. Liao, Y. Sohn, M. Riutin, A. Cecconello, W. J. Parak, R. Nechushtai and I. Willner, *Adv. Funct. Mater.*, 2016, **26**, 4262-4273.
38 C. C. Kloss, M. Condomines, M. Cartellieri, M. Bachmann and M. Sadelain, *Nat. Biotechnol.*, 2013, **31**, 71-75.
39 M. I. Shukoor, M. O. Altman, D. Han, A. T. Bayrac, I. Ocsoy, Z. Zhu and W. H. Tan, *ACS Appl. Mater. Interfaces*, 2012, **4**, 3007-3011.
40 H. C. Yeh, J. Sharma, I.-M. Shih, D. M. Vu, J. S. Martinez and J. H. Werner, *J. Am. Chem. Soc.*, 2012, **134**, 11550-11558.
41 K. Szaciłowski, *Chem. Rev.*, 2008, **108**, 3481-3548.
42 F. Pu, E. Ju, J. S. Ren and X. G. Qu, *Adv. Mater.*, 2014, **26**, 1111-1117.
43 G. Seelig, D. Soloveichik, D. Zhang and E. Winfree, *Science*, 2006, **314**, 1585-1588.
44 S. Gibilisco, The Illustrated Dictionary of Electronics, Gibilisco S. ed., McGraw-Hill: *New York*, 2001, **81**.
45 Y. Q. Liu, J. T. Ren, Y. A. Qin, J. Li, J. Y. Liu and E. K. Wang, *Chem. Commun.*, 2012, **48**, 802-804.
46 D. Q. Fan, K. Wang, J. B. Zhu, Y. Xia, Y. C. Han, Y. Q. Liu and E. K. Wang, *Chem. Sci.*, 2015, **6**, 1973-1978.
47 S. S. Oh, K. Plakos, X. H. Lou, Y. Xiao and H. T. Soh, *Proc. Natl. Acad. Sci. USA*, 2010, **107**, 14053-14058.
48 H. L. Li, J. Y. Liu, Y. X. Fang, Y. N. Qin, S. L. Xu, Y. Q. Liu and E. K. Wang, *Biosens. Bioelectron.*, 2013, **41**, 563-568.
49 S. L. Xu, H. L. Li, Y. Q. Miao, Y. Q. Liu and E. K. Wang, *NPG Asia Materials*, 2013, **5**, e76.
50 J. Andréasson and U. Pischel, *Chem. Soc. Rev.*, 2010, **39**, 174-188.
51 C. N. Yang, C. Y. Hsu and Y. C. Chuang, *Chem. Commun.*, 2012, **48**, 112-114.
52 C. T. Wu, K. Wang, D. Q. Fan, C. Y. Zhou, Y. Q. Liu and E. K. Wang, *Chem. Commun.*, 2015, **51**, 15940-15943.
53 J. Andréasson, S. D. Straight, S. Bandyopadhyay, R. H. Mitchell, T. A. Moore, A. L. Moore and D. Gust, *Angew. Chem. Int. Ed.*, 2007, **46**, 958-961.
54 H. X. Yuan, Z. Liu, L. B. Liu, F. T. Lv, Y. L. Wang and S. Wang, *Adv. Mater.*, 2014, **26**, 4333-4338.
55 S. I. Stoeva, J. S. Lee, J. E. Smith, S. T. Rosen and C. A. Mirkin, *J. Am. Chem. Soc.*, 2006, **128**, 8378-8379.
56 J. T. Petty, J. Zheng, N. V. Hud and R. M. Dickson, *J. Am. Chem. Soc.*, 2004, **126**, 207-5212.



View Article Online
DOI: 10.1039/C7SC05246D

# Table of Contents

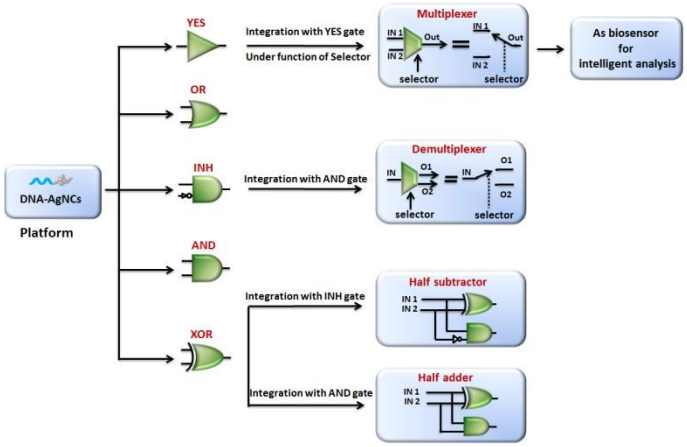


A set of basic logic gates were constructed on a simple and universal DNA-AgNCs platform, which were further integrated into advanced logic circuits for DNA computing and biosensing.